Luminescence of the Red Modification of Single-Crystal $Pt(bpy)Cl_2$ (bpy: 2,2′-Bipyridine)

Evidence for Strong Inter-Complex Coupling

M. Weiser-Wallfahrer and G. Gliemann*

Institut für Physikalische und Theoretische Chemie, Universität Regensburg, D-8400 Regensburg, F.R.G.

Dedicated to Prof. Dr. Dirk Reinen on the occasion of his 60th birthday

Z. Naturforsch. **45b**, 652–657 (1990); received December 1, 1989

Luminescence, Single-Crystal $Pt(bpy)Cl_2$, Inter-Complex Coupling

The polarized optical emission (energy, intensity, lifetime) of the red modification of single-crystal $Pt(bpy)Cl_2$ as a function of temperature ($1.9 \leq T \leq 298$ K) and homogeneous magnetic fields ($0 \leq H \leq 6$ T), and the temperature dependence of the polarized optical absorption are reported. Analysis of the spectra indicates a strong inter-complex coupling giving rise to electronic band structures and self-trapped states.

Introduction

The photophysics and photochemistry of square-planar d^8 complexes have attracted great attention during the last years, since the character of their lowest excited electronic states (LF, LC, MLCT or LMCT) can be varied distinctly by appropriate choice of the ligands and the central metal [1–15]. Special interest has been focused to cyclometallated complexes and related compounds, since several of these systems can be used as light emission sensitizers (LES), as light absorption sensitizers (LAS) or for the interconversion between light energy and chemical energy [1–8].

In their crystalline form several of these complexes exhibit remarkable optical features owing to special properties of their electronic systems. The latter depend strongly on the structural arrangement of the complexes in the solid. An instructive example is yielded by the compound $[Pt(bpm)(CN)_2]$, which can be crystallized as $[Pt(bpm)(CN)_2]\cdot H_2O$ [16], $[Pt(bpm)(CN)_2]\cdot DMF$ [17], or $[Pt(bpm)(CN)_2]$ [18], with bpm = 2,2′-bipyrimidine. In the crystals of all three systems the $[Pt(bpm)(CN)_2]$ units are stacked forming mutually parallel columns. The intra-columnar Pt–Pt distances, however, are different for the three systems. As a consequence, their optical absorption and emission spectra vary completely corresponding to the different strength of the inter-complex coupling.

The compound $Pt(bpy)Cl_2$ forms two types of crystals, a red and a yellow form [19–21]. In the red modification the nearly planar $Pt(bpy)Cl_2$ units are stacked forming linear columns with a Pt–Pt distance of 3.45 Å. The yellow modification, however, shows no columnar structure and the Pt atoms are distinctly more distant (~4.5 Å). From these structural variations considerably different inter-complex couplings are expected, which will be reflected in the optical spectra. The purpose of this paper is to report the polarized absorption and emission of the red modification as functions of the temperature and of applied magnetic fields. Finally, an energy level system of the electronic states of the red modification will be outlined, which supplies an interpretation of the optical properties on the basis of the crystal structure.

Experimental

$Pt(bpy)Cl_2$ was prepared with reference to a method described by Textor and Oswald [20]. In a first step an aqueous solution of K_2PtCl_4 (2.41 mmol) is reacted with 2,2′-bipyridine (2.50 mmol). By dropwise addition of 5 ml 2 N HCl and heating of the solution, a yellow needle like precipitate results. For purification the precipitate is washed several times with bidestilled water, ethanol, and ether. By recrystallization from DMF and further purification, $Pt(bpy)Cl_2$ crystals of the yellow modification are obtained. In a second step, 0.05 g of these crystals are dissolved in 10 ml pyridine (at

* Reprint requests to Prof. Dr. G. Gliemann.

Verlag der Zeitschrift für Naturforschung, D-7400 Tübingen
0932–0776/90/0500–0652/$ 01.00/0

~55 °C). By slow evaporation the solution is reduced to about 2 ml. After addition of 30 ml CCl_4 a precipitate of red needle shaped crystals appears. The precipitate is collected by filtration, washed thoroughly with CCl_4, and dried at room temperature.

The apparatus for the polarized absorption spectroscopy, the polarized emission spectroscopy and lifetime measurements have been described in [22] and [23]. The 364 nm line of an argon-ion laser was used as the excitation source for the cw spectra and the 488 nm line of a cavity dumped dye laser system for the lifetime measurements.

Results

Absorption

The absorption spectra of the red modification of single-crystal $Pt(bpy)Cl_2$ are shown in Fig. 1. The extinction coefficient of the **E**||**a** polarized component at $\bar{\nu} \leq 24{,}000\ cm^{-1}$ is much larger than that of the **E** ⊥ **a** spectrum ($\varepsilon_\perp \approx 2500\ M^{-1}\ cm^{-1}$), so that with **E**||**a** polarization only the low-energy flank of the absorption could be measured. **E** and **a** are the orientations of the electric field vector of the light and of the needle axis, respectively. The **E** ⊥ **a** absorption spectrum at $\bar{\nu} \leq 24{,}000\ cm^{-1}$ is composed of four bands I, ..., IV. With decreasing temperature from $T = 298$ K to 10 K these bands become more pronounced and the maxima of the bands I and II are red shifted by $\Delta\bar{\nu} \sim 1100\ cm^{-1}$, the spectral positions of the bands III and IV, however, are independent of temperature. A fine structure of the absorption spectrum as observed with the yellow modification, *cf.* Ref. [24], could not be detected with the red form.

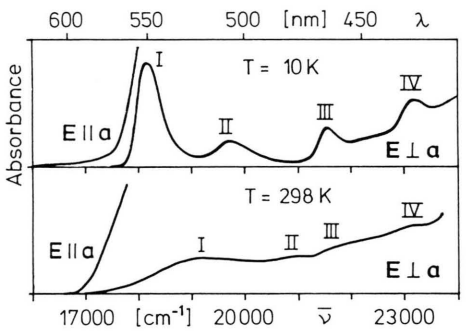

Fig. 1. **E**||**a** and **E**⊥**a** polarized absorption spectra of the red modification of single-crystal $Pt(bpy)Cl_2$ (thickness ≈ 10 μm) at $T = 10$ and 298 K.

Emission

In contrast to the yellow form the red modification of $Pt(bpy)Cl_2$ emits already at room temperature. As shown in Fig. 2 for $H = 0$, the **E**||**a** and the **E**⊥**a** emission spectra consist of one band each. The maximum of the **E**||**a** emission band is higher in energy by ~235 cm^{-1} than that of the **E**⊥**a** band. At $T = 1.9$ K the intensity ratio $I_\perp / I_{||}$ is about 3. With increasing temperature the intensity ratio decreases to ~1 at $T = 160$ K and to ~0.3 at room temperature. Between $T = 1.9$ K and ~20 K the maximum of the **E**⊥**a** polarized emission is blue shifted by $\Delta\bar{\nu} \approx 220\ cm^{-1}$, whereas the spectral position of the **E**||**a** emission is not changed. At further increase of the temperature to $T = 298$ K, the energies of the emission maxima grow by ~800 and ~1100 cm^{-1} for **E**⊥**a** and **E**||**a** polarization, respectively.

The **E**⊥**a** polarized emission of the red form exhibits a mono-exponential decay, and between $T = 1.9$ and 80 K the lifetime decreases from ~120 μs to ~0.6 μs. The decay behavior of the **E**||**a** emission could not be determined quantitatively, since the corresponding lifetime has been proven to be shorter than the limit of detection of our apparatus ($\tau \approx 0.3$ ns).

The **E**⊥**a** polarized emission can be influenced by a homogeneous magnetic field **H** with **H**⊥**a**, *cf.*

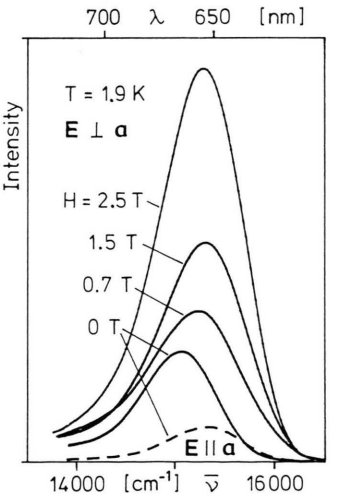

Fig. 2. **E**||**a** and **E**⊥**a** polarized emission spectra of the red modification of single-crystal $Pt(bpy)Cl_2$ at $T = 1.9$ K. For **E**⊥**a** polarization the spectrum at different magnetic field strengths with **H**⊥**a** is shown. $\lambda_{exc} = 364$ nm.

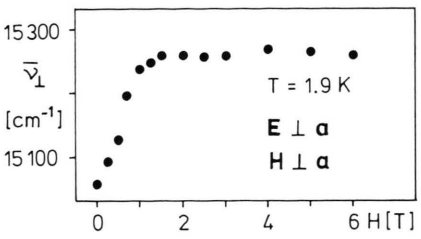

Fig. 3. The wavenumber $\bar{\nu}_\perp$ of the **E**⊥**a** emission maximum of the red modification of single-crystal Pt(bpy)Cl_2 as a function of the magnetic field strength H. T = 1.9 K. λ_{exc} = 364 nm. **H**⊥**a.**

Fig. 2. With increasing magnetic field strength between $H = 0$ and $H = 1.5$ T the emission maximum is blue shifted by $\Delta\bar{\nu} \sim 205$ cm^{-1}, as shown in Fig. 3. At $1.5 \leq H \leq 6$ T the emission energy is nearly independent of the field strength. Furthermore, raising the field strength from $H = 0$ to 6 T yields an increase of the quantum yield by a factor of ~7 and a reduction of the emission lifetime from $\tau \sim 120$ μs to 30 μs. The log-log plot of $1/\tau_H - 1/\tau_0$ *versus* H yields a straight line with a slope of about 2, *cf.* Fig. 4. For the **E**||**a** polarized emission no magnetic field effect has been observed with **H**⊥**a.** Magnetic fields with **H**||**a** do not affect the emission in any way.

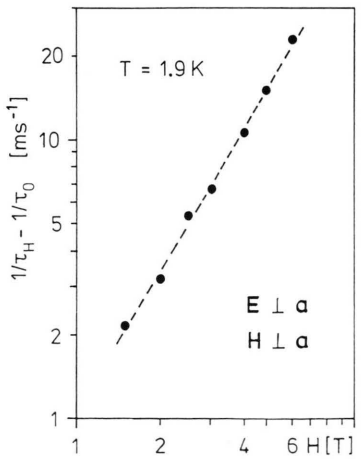

Fig. 4. Change of the radiative deactivation rate of the red modification of single-crystal Pt(bpy)Cl_2 as a function of magnetic field strength. τ_H and τ_0 are the emission lifetimes at magnetic field strengths H and $H = 0$, respectively. λ_{exc} = 488 nm.

Discussion

The crystal structure of the red modification of Pt(bpy)Cl_2 has been reported by Textor and Oswald [20] and by Osborn and Rogers [21]. The nearly square-planar molecules have C_{2v} symmetry and crystallize according to the ortho-rhombic space group Cmcm.

In the crystal the molecules are arranged in columns, which are parallel to the crystallographic a axis (= needle axis), as indicated in Fig. 5. Neighboring molecules of a column are 3.40 Å apart; they are mutually rotated by an angle of 180° around the molecular x axis. The Pt atoms of each column form a zig-zag chain; the deviation from linearity, however, is very small (~±0.2 Å).

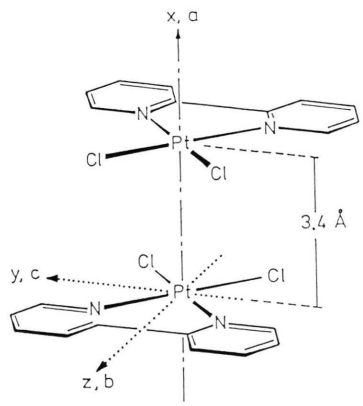

Fig. 5. Part of the columnar structure of the red modification of Pt(bpy)Cl_2, schematic [7].

In the ligand field of symmetry C_{2v}, the energy order of the Pt d-orbitals of a single complex molecule is expected as follows

$$a_1(x^2) < b_1(xz),\ a_2(xy) < a_1(y^2-z^2) \ll b_2(yz)$$

The HOMO and LUMO of the heterocyclic ligand transform according to $a_2(\pi)$ and $b_1(\pi^*)$, respectively. For symmetry reasons the ligand state $b_1(\pi^*)$ can mix with the energetically nearby metal $6p_x$ state, yielding the LUMO $b_1(\pi^*, x)$ of the complex molecule. Correspondingly, the HOMO of the complex molecule, $a_2(\pi, xy)$, is a mixture of the HOMO $a_2(\pi)$ of the bpy ligand and of the metal d_{xy} state.

Because of the short intra-columnar Pt–Pt distance in the red modification of single-crystal Pt(bpy)Cl_2, neighboring complex molecules interact and corresponding orbitals form energy bands. The orbitals $a_1(x^2)$ and $b_1(\pi^*, x)$ having maximum extension along the columnar axis, yield relatively large band splittings. As a result, the upper edge of the $a_1(x^2)$ band forms the HOMO of the crystal, whereas the lower edge of the $b_1(\pi^*, x)$ band represents the LUMO.

If electron interaction and spin-orbit coupling (double group C'_{2v}) are taken into account, the ground electronic state of the crystal is $A'_1(^1A_1)$. The lowest excited electronic bands are due to the transition $a_1(x^2) \rightarrow b_1(\pi^*, x)$ and can be classified according to the representations $B'_1(^1B_1)$ and A'_1, A'_2, $B'_2(^3B_1)$.

Absorption

With regard to its polarization and its high extinction the **E**||**a** polarized absorption (*cf.* Fig. 1) can be assigned to the symmetry and spin allowed band-band transition $A'_1(^1A_1) \rightarrow B'_1(^1B_1)$. Correspondingly, the low-energy absorption band I with **E**⊥**a** polarization belongs to the two symmetry allowed singlet-triplet band-band transitions $A'_1(^1A_1) \rightarrow A'_1, B'_2(^3B_1)$. The relatively large extinction coefficient of $\varepsilon_\perp \approx 2500\ M^{-1}\ cm^{-1}$ indicates a strong spin-orbit coupling, due to the relatively large admixture of metal character in the involved electronic states, the energy separation of the spin-orbit components A'_1 and B'_2, however, is small compared with the half-width of band I ($\Delta\bar{\nu}_{1/2} \sim 500\ cm^{-1}$ at $T = 10$ K). With increasing temperature the intra-chain Pt–Pt distances grow and, thus, the splitting of the electronic bands is reduced. As a consequence the spectral positions of the corresponding band-band transitions are blue shifted. For the **E**⊥**a** polarized band I the blue shift between $T = 10$ and 298 K is $\Delta\bar{\nu} \approx 1100\ cm^{-1}$. Similar values have been observed for single-crystal tetracyanoplatinates(II) [25]. A blue shift of the strong **E**||**a** polarized absorption could not be quantified, since the spectral position of the observable low-energy flank of this absorption band can be influenced both by the called blue shift of the band maximum and by a broadening of the band. The low-energy transition $A'_1(^1A_1) \rightarrow A'_2(^3B_1)$ is symmetry and spin forbidden and cannot be detected in the absorption spectrum.

The maximum II in the **E**⊥**a** polarized absorption spectrum, *cf.* Fig. 1, is probably a vibrational satellite of band I, due to a totally symmetric vibration. This assignment is confirmed by the similar temperature dependence of the spectral positions and of the extinctions of the bands I and II. For the origin of the absorption maxima III and IV, which exhibit a different behavior, we have no definitive interpretation.

Emission

The emission spectra can be traced back to radiative deactivations both of free exciton states of excited columns of complexes and of self-traps formed by electronically excited single complexes or by excited small clusters of complexes, being stabilized by relaxation processes. To realize several of the emission properties an energy barrier between the free exciton states and the self-traps has to be postulated, *cf.* Fig. 6. The energy order of the self-trapped states can be deduced from the experimental results, *vide infra*, as $E(A'_2) < E(A'_1) \approx E(B'_2)$.

At $T = 1.9$ K, mainly the free exciton states and the lowest self-trapped state $A'_2(^3B_1)$ are occupied, and the energy barrier prevents a thermal repopulation between them. Thus, the radiative deactivation of the exciton state $B'_1(^1B_1)$ yields the spontaneous **E**||**a** emission exhibiting a very short lifetime ($\tau < 0.3$ ns). Since a radiative deactivation from the A'_2 directly to the ground electronic state A'_1 is forbidden, the deactivation is due to the vibronic transition $A'_2(^3B_1) \rightarrow A'_1(^1A_1) + \alpha_2, \beta_1$ with α_2 and β_1 the symmetry characters of the accepting vi-

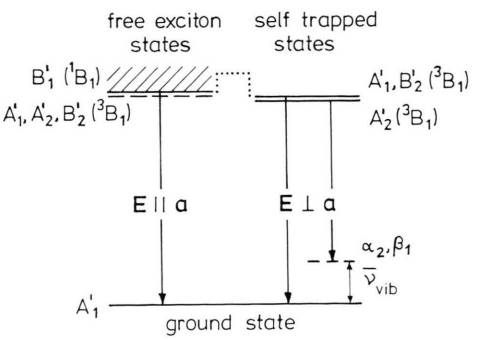

Fig. 6. Proposed energy-level diagram of the emitting states of Pt(bpy)Cl_2 (red modification) (schematic). Left-hand side: free exciton states. Right-hand side: self-trapped states.

brations. This transition is **E**⊥**a** polarized and yields the emission band at $\bar{\nu}_\perp \approx 15{,}060\ cm^{-1}$. With increasing temperature the states A'_1 and B'_2 (of $^3B_1$ parentage) are more and more thermally populated. These states can be radiatively deactivated directly to the ground electronic state $A'_1(^1A_1)$. The corresponding transition has an energy higher by $\Delta\bar{\nu}_T = \Delta E + \bar{\nu}_{vib}$ than the vibronic transition, mentioned above. ΔE is the energy difference between the lowest excited states and $\bar{\nu}_{vib}$ is the energy quantum of the accepting vibration. The blue shift of $\Delta\bar{\nu} \sim 220\ cm^{-1}$ observed for the **E**⊥**a** emission between $T = 1.9$ and 20 K is a lower limit of $\Delta\bar{\nu}_T$, since at $T = 1.9$ K the emission from the states A'_1, $B'_2(^3B_1)$ cannot be neglected completely. The temperature dependence of the lifetime of the **E**⊥**a** emission confirms the outlined model sufficiently, if for ΔE a value of about $15\ cm^{-1}$ is assumed. The additional blue shift at $T > 20$ K is owing to the thermal increase of the intra-chain Pt–Pt distance.

The **E**||**a** polarized emission is symmetry and spin allowed. Therefore, a blue shift between $T = 1.9$ and 20 K, as observed for the **E**⊥**a** emission, does not occure with the **E**||**a** emission. The temperature induced blue shift of the **E**||**a** emission at $T > 20$ K, however, is caused also by the thermal expansion of the crystal. The value of the blue shift at $T > 20$ K is different for the **E**||**a** and **E**⊥**a** emission because of the different nature of the emitting states.

The temperature induced decrease of the intensity ratio $I_\perp/I_{||}$ from ~3 ($T = 1.9$ K) to ~0.3 ($T = 298$ K) can be traced back to the effect of the energy barrier. With temperature increase the barrier can be thermally surmounted, which leads to a relative decrease of the **E**⊥**a** intensity.

The effects of homogeneous magnetic fields **H** can be described straightforwardly on the basis of the energy level diagram of the self-trapped states shown in Fig. 7. Magnetic fields with **H**||**z** (**H**||**y**) reduce the symmetry of the system to C_2 (C_s). In both cases the state $A'_2(^3B_1)$ mixes with one of the triplet states A'_1 and B'_2, respectively, and the radiative deactivation of the $A'_2(^3B_1)$ to the vibrationally non-excited ground state becomes allowed. This transition is blue shifted by $\Delta\bar{\nu}_H = \bar{\nu}_{vib}$ compared with the low-temperature vibronic transition at zero field. The experimental value $\Delta\bar{\nu} \sim 205\ cm^{-1}$ is a lower limit of $\bar{\nu}_{vib}$. The observed magnetic field induced increase of the emission intensity and of the rate constant, $1/\tau_H - 1/\tau_0 \sim H^2$, confirms the proposed model and can be explained on the basis of quantum mechanical perturbation theory [26]. By magnetic fields **H**||**a** the components $A'_1(^3B_1)$ and $B'_2(^3B_1)$ mix mutually but not with the state $A'_2(^3B_1)$. Therefore, with **H**||**a** a magnetic field effect on the low-temperature **E**⊥**a** emission cannot be observed.

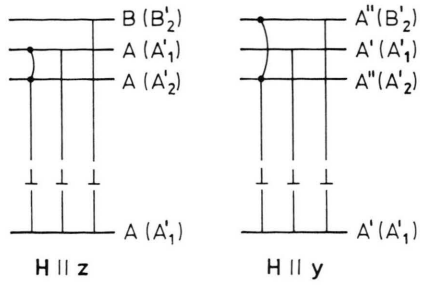

Fig. 7. Proposed energy-level diagram of Pt(bpy)Cl_2 (red modification) and electric dipole transition at magnetic fields (schematic). Left-hand side: **H**||**z** (symmetry C_2). Right-hand side: **H**||**y** (symmetry C_s).

This research has been supported by the Fonds der Chemischen Industrie.

[1] S. Sprouse, K. A. King, and R. J. Watts, J. Am. Chem. Soc. **106,** 6647 (1984).
[2] Y. Ohsawa, S. Sprouse, K. A. King, M. K. DeArmond, K. W. Hank, and R. J. Watts, J. Phys. Chem. **91,** 1047 (1987).
[3] M. Maestri, D. Sandrini, V. Balzani, U. Maeder, and A. v. Zelewsky, Inorg. Chem. **26,** 1323 (1987).
[4] U. Maeder, T. Jenny, and A. v. Zelewsky, Helv. Chim. Acta **69,** 1085 (1986).
[5] S. Bonafede, M. Ciano, F. Bolletta, V. Balzani, L. Chassot, and A. v. Zelewsky, J. Phys. Chem. **90,** 3836 (1986).
[6] C. Cornioley-Deuschel und A. v. Zelewsky, Inorg. Chem. **26,** 3354 (1987).
[7] R. Schwarz, G. Gliemann, Ph. Jolliet, and A. v. Zelewsky, Inorg. Chem. **28,** 742 (1989).
[8] R. Schwarz, G. Gliemann, Ph. Jolliet, and A. v. Zelewsky, Inorg. Chem. **28,** 1053 (1989).
[9] L. Bär, G. Gliemann, L. Chassot, and A. v. Zelewsky, Chem. Phys. Lett. **123,** 264 (1986).
[10] L. Chassot, E. Müller, and A. v. Zelewsky, Inorg. Chem. **23,** 4249 (1984).
[11] V. Balzani, F. Bolletta, M. T. Gandolfi, and M. Maestri, Top. Curr. Chem. **75,** 1 (1978).
[12] G. A. Crosby, Acc. Chem. Res. **8,** 231 (1975).
[13] G. A. Crosby, J. Chem. Educ. **60,** 791 (1983).
[14] R. J. Watts, G. A. Crosby, and J. L. Sansegret, Inorg. Chem. **11,** 1474 (1972).
[15] R. J. Watts and G. A. Crosby, Chem. Phys. Lett. **13,** 619 (1972).
[16] J. Biedermann, G. Gliemann, U. Klement, K.-J. Range, and M. Zabel, Inorg. Chim. Acta **69,** 63 (1989).
[17] J. Biedermann, G. Gliemann, U. Klement, K.-J. Range, and M. Zabel, Inorg. Chim. Acta, in press.
[18] J. Biedermann, G. Gliemann, U. Klement, K.-J. Range, and M. Zabel, Inorg. Chem., in press.
[19] G. T. Morgan and F. H. Burstall, J. Chem. Soc. **1934,** 965.
[20] M. Textor and H. R. Oswald, Z. Anorg. Allg. Chem. **407,** 244 (1984).
[21] R. S. Osborn and D. Rogers, J. Chem. Soc. Dalton Trans. **1974,** 1002.
[22] W. Tuszynski and G. Gliemann, Ber. Bunsenges. Phys. Chem. **89,** 940 (1985).
[23] I. Hidvegi, W. v. Ammon, and G. Gliemann, J. Chem. Phys. **76,** 4361 (1982); W. v. Ammon, I. Hidvegi, and G. Gliemann, ibid. **80,** 2837 (1984).
[24] M. Weiser-Wallfahrer and G. Gliemann, to be published.
[25] G. Gliemann and H. Yersin, Struct. Bonding **62,** 87 (1985).
[26] G. Gliemann, Comments Inorg. Chem. **5,** 263 (1986).